

Non-classical Rotational Inertia in a Two-dimensional Bosonic Solid Containing Grain Boundaries

Chandan Dasgupta*

*Centre for Condensed Matter Theory, Department of Physics,
Indian Institute of Science, Bangalore 560012, India*

Oriol T. Valls†

School of Physics and Astronomy, University of Minnesota, Minneapolis, Minnesota 55455

(Dated: June 16, 2010)

We study the occurrence of non-classical rotational inertia (NCRI) arising from superfluidity along grain boundaries in a two-dimensional bosonic system. We make use of a standard mapping between the zero-temperature properties of this system and the statistical mechanics of interacting vortex lines in the mixed phase of a type-II superconductor. In the mapping, the liquid phase of the vortex system corresponds to the superfluid bosonic phase. We consider numerically obtained polycrystalline configurations of the vortex lines in which the microcrystals are separated by liquid-like grain boundary regions which widen as the vortex system temperature increases. The NCRI of the corresponding zero-temperature bosonic systems can then be numerically evaluated by solving the equations of superfluid hydrodynamics in the channels near the grain boundaries. We find that the NCRI increases very abruptly as the liquid regions in the vortex system (equivalently, superfluid regions in the bosonic system) form a connected, system-spanning structure with one or more closed loops. The implications of these results for experimentally observed supersolid phenomena are discussed.

I. INTRODUCTION

The observation^{1,2} of non-classical rotational inertia (NCRI) in torsional oscillation experiments on solid ^4He created a great deal of interest³ in the possibility of occurrence of a “supersolid” phase in which crystalline order and superfluidity coexist. Considerable subsequent work has sustained this interest. The occurrence of NCRI in solid ^4He has been confirmed in many experiments^{4–9} and the dependence of the measured NCRI fraction (NCRIF) on various factors, such as the method of sample growth, its annealing, frequency and amplitude of the torsional oscillator and the amount of ^3He impurities present, have been studied in great detail. However, despite these extensive studies, the microscopic origin of the observed NCRI signal remains quite controversial. In particular, it is not clear whether the superfluid component in supersolid ^4He is distributed uniformly throughout the sample, or present only near structural defects such as dislocations and grain boundaries. A suggestion that the observed phenomena were related to an old theoretical proposal¹⁰ of superfluidity arising from mobile zero-point vacancies in the crystal has been contradicted by results of quantum Monte Carlo simulations^{11,12} that show that the concentration of vacancies is too low to account for the measured NCRIF. On the other hand, the observed dependence⁴ of the magnitude of the NCRIF on the quality of the sample (samples with higher degree of crystalline order exhibit smaller NCRIF) argues in favor of a mechanism of superfluidity in which defects play a major role. An important role for the defects is also indicated by the observation^{9,13} of a close correspondence between the onset of NCRI and an increase of the shear modulus of the solid, and by an enhancement of both these effects

when the concentration of ^3He impurities is increased. It has been suggested¹³ that both the occurrence of NCRI and the simultaneous increase in the shear modulus arise from a stiffening of a network of dislocation lines, and that this stiffening is assisted by ^3He impurities which pin the dislocation lines by binding to them.

The question of whether the experimentally observed supersolid behavior in ^4He can arise from the presence of structural defects has been investigated, on the theoretical side, in quantum Monte Carlo studies^{14–16} that show that superfluidity can indeed occur along grain boundaries and in the cores of dislocations. There have been a few attempts^{17–21} to calculate the macroscopic properties (such as the NCRIF) of a system in which superfluidity occurs along a network of grain boundaries or dislocation lines. Since these structural defects form disordered complex networks, a calculation of the rotational inertia of a superfluid confined in a network of irregular-shaped channels is necessary for understanding whether a defect-based mechanism can provide a consistent explanation of the observed results. To our knowledge, no such calculation for realistic defect network structures currently exists in the literature.

In this paper we study the possibility of occurrence of “supersolid” behavior, similar to that observed in solid ^4He , arising from superfluidity along grain boundaries in a two-dimensional bosonic system. We make use of a well-known mapping^{22–24} between the statistical mechanics of a system of interacting vortex lines in the mixed phase of type-II superconductors and the zero-temperature quantum mechanics of a *two-dimensional* system of bosons. Specifically, we consider a highly anisotropic layered superconductor in the presence of a magnetic field perpendicular to the layers. The system

then consists of a collection of vortex lines oriented, on the average, normal to the layers. The statistical mechanics of these vortex lines can be mapped^{22–24} onto the quantum mechanics of a two-dimensional system of interacting bosons at zero temperature. The mapping can also be used if a small concentration of columnar pinning centers normal to the layers is present in the vortex system. In that case, the equivalent bosonic system contains a small concentration of randomly located point pinning centers that produce a random external potential for the bosons. In this mapping, the liquid phase of the vortex system corresponds to the superfluid phase of the bosons. The equilibrium properties of the vortex system, both with and without columnar pinning, have been investigated in a large number of theoretical^{22–24}, experimental^{25–27} and numerical^{28–32} studies. These results establish, as we will show below, that the zero-temperature, two-dimensional, interacting bosonic system with random pinning centers exhibits a polycrystalline state with superfluidity along grain boundaries over a suitable range of system parameters.

Our earlier studies^{28–30} of the vortex system in the presence of columnar pins provide us with several realistic configurations of the network of grain boundaries. We find that some of these polycrystalline states survive as metastable states when the random pinning potential is turned off, as explained below. This case maps then onto the impurity-free bosonic system, which is similar to the experimentally studied ⁴He case. We then study the NCRIF arising from the superfluid regions along the grain boundaries by numerically solving the equations of superfluid hydrodynamics^{33,34} in the geometry specified by the superfluid channels in the sample. This allows us to determine the NCRIF as a function of system parameters. At low temperatures (meaning the temperature of the vortex system, *not* that of the two-dimensional bosonic system), the liquid regions (superfluid regions in the equivalent two-dimensional system of bosons) near the grain boundaries are completely absent or small, and the NCRIF is vanishingly small. As the temperature is increased towards the melting temperature of the vortex lattice in the absence of any pinning, a kind of “pre-melting” occurs near the grain boundaries, so that the area covered by the liquid regions increases. This increases the connectivity of the network of liquid channels and causes the NCRIF to increase as the channels open up throughout the entire sample. However, the NCRIF remains vanishingly small as long as the liquid regions remain isolated from one another. Our main result is that the NCRIF exhibits a sharp jump to a measurable value of a few percent when the growing liquid regions percolate across the system to form one or more closed channels of size comparable to the size of the system. The behavior of the NCRIF as a function of the temperature of the vortex system is qualitatively similar to that seen in the experiments on ⁴He. Our work, thus, shows that supersolid behavior similar to that observed in solid ⁴He can occur from superfluidity in grain boundaries in

a two-dimensional system of bosons for an appropriate choice of parameters.

The rest of the paper is organized as follows. In section II, we provide the details of the vortex-to-boson mapping used in our work, define the model we consider and describe the numerical methods used in our calculations. The results of our study are described in detail in section III. Section IV contains a discussion of the implications of our results in the context of current research on supersolidity in ⁴He.

II. MAPPING, MODELS AND METHODS

In this section, we first describe in detail the mapping between the statistical mechanics of a collection of vortex lines and the zero-temperature quantum mechanics of a two-dimensional system of bosons. We then discuss how existing results for the vortex system can be used to infer the occurrence of a “supersolid” phase with superfluidity along grain boundaries in the bosonic system under suitable conditions. In our study, information about the behavior of the bosonic system is obtained, through the vortex-boson mapping, from calculations carried out for the vortex system. At the end of this section, we provide some details of the model used in our study of the vortex system and the method of calculation we have used.

A. Mappings and Models

It is well established^{22–24} that the partition function of a system of interacting vortex lines can be written as that of a two-dimensional system of interacting bosons. We review here only the necessary details. Let us consider a system of N vortex lines in a type-II superconductor in the mixed phase, with the magnetic field in the z -direction. We also assume that N_p columnar pinning centers oriented along the z direction may be present in the sample (this random pinning potential will be turned off in the numerical work described below). Let the two-dimensional vector $\mathbf{r}_j(z)$ denote the transverse position of the j -th vortex line in the xy -plane at z ($0 \leq z \leq L$ where L is the thickness of the sample in the z -direction). The free energy of the system of vortex lines has the form

$$\begin{aligned}
 F_N = & \frac{1}{2} \sum_{j=1}^N \epsilon \int_0^L \left| \frac{d\mathbf{r}_j(z)}{dz} \right|^2 dz \\
 & + \frac{1}{2} \sum_{i \neq j} \int_0^L V(|\mathbf{r}_i(z) - \mathbf{r}_j(z)|) dz \\
 & + \sum_{j=1}^N \int_0^L V_d(\mathbf{r}_j(z)) dz.
 \end{aligned} \tag{2.1}$$

Here, ϵ is the tilt modulus of the vortex lines, $V(r)$ is the interaction potential between two vortex lines separated by transverse distance r , and $V_d(\mathbf{r})$ is a pinning

potential produced by the columnar pinning centers (for columnar pins oriented in the z -direction, the pinning potential does not depend on z). We assume periodic boundary condition in the z -direction, which implies that

the positions $\{\mathbf{r}_j(0)\}$ and $\{\mathbf{r}_j(L)\}$ at the two ends of the sample must match modulo a permutation. The partition function of the system of vortex lines at temperature T is then given by

$$Z_v(T) = \frac{1}{N!} \sum_P \prod_{j=1}^N \int_{\mathbf{r}_j(L)=\mathbf{r}_{P(j)}(0)} \mathcal{D}\{\mathbf{r}_j(z)\} \exp[-F_N/T], \quad (2.2)$$

where the functional integrals are over all vortex-line configurations that satisfy the boundary conditions $\mathbf{r}_j(L) = \mathbf{r}_{P(j)}(0)$ for all j , P representing a permutation of the indices $1, 2, \dots, N$.

To see the connection of this problem with the quantum mechanics of bosons, let us consider a two-dimensional system of N identical bosonic particles of mass m , with pairwise interactions given by the potential $V(r)$, in the presence of an external impurity potential $V_d(\mathbf{r})$. In the path integral representation, the partition function of this system at temperature T_b can be written as

$$Z_b(T_b) = \frac{1}{N!} \sum_P \prod_{j=1}^N \int_{\mathbf{r}_j(\Lambda)=\mathbf{r}_{P(j)}(0)} \mathcal{D}\{\mathbf{r}_j(\tau)\} \exp \left[-\frac{1}{\hbar} \left\{ \sum_{j=1}^N \int_0^\Lambda \frac{m}{2} \left| \frac{d\mathbf{r}_j(\tau)}{d\tau} \right|^2 d\tau \right. \right. \\ \left. \left. + \frac{1}{2} \sum_{i \neq j} \int_0^\Lambda V(|\mathbf{r}_i(\tau) - \mathbf{r}_j(\tau)|) d\tau + \sum_{j=1}^N \int_0^\Lambda V_d(\mathbf{r}_j(\tau)) d\tau \right\} \right], \quad (2.3)$$

where $\mathbf{r}_j(\tau)$ now represents the position of the j -th boson at “imaginary time” τ and $\Lambda = \hbar/T_b$. A comparison of this expression with that in Eq. (2.2) shows that the two are the same when one makes the identifications

$$\epsilon \rightarrow m, \quad T \rightarrow \hbar, \quad L \rightarrow \Lambda = \hbar/T_b. \quad (2.4)$$

Thus, the thermodynamic limit, $L \rightarrow \infty$, in the vortex system corresponds to the zero temperature ($T_b = 0$) limit in the boson system. The tilt modulus of the vortex lines plays the role of the mass of the bosons and the temperature T of the vortex system plays the role of \hbar . The pairwise interaction $V(r)$ in the system of bosons is the same as that between two vortex lines and the external potential $V_d(\mathbf{r})$ is also the same in the two systems. The interaction between two straight vortex lines parallel to each other is repulsive and its dependence of the transverse separation is given by $V(r) \propto K_0(r/\lambda)$ where K_0 is a Bessel function and λ the in-plane London penetration depth of the superconductor. Thus, the pair interaction potential in the corresponding boson problem is repulsive, logarithmic in r for r much smaller than λ , and falls off exponentially as $\sim \exp(-r/\lambda)$ when r is larger than λ . Liquid phases in the vortex system correspond to superfluid bosonic phases, while vortex crystalline phases correspond to a bosonic crystal.

This mapping between the two systems allows us to draw certain conclusions about the behavior of the two-dimensional bosonic system from the wealth of information available from existing experimental^{25–27} and numerical^{28–32} studies of the mixed phase of type-II layered superconductors (high-temperature cuprate superconductors in particular) in the presence of random

columnar pinning centers oriented parallel to the magnetic field which is perpendicular to the layers. These studies establish that when the concentration of pinning centers is small compared to that of vortex lines, the vortex system exhibits a Bose glass (BoG) phase at low temperatures, and a vortex liquid phase at high temperatures. In the vortex-boson mapping, the vortex liquid phase corresponds to the superfluid phase of the two-dimensional bosonic system. Both experiments²⁵ and numerical studies^{28–30} show that the BoG phase in the vortex system has a polycrystalline structure with grain boundaries separating crystalline domains (see, for example, Fig. 2 of Ref. 25 and Fig. 1 of Ref. 28). Experiments also show the existence of a “vortex nanoliquid” phase^{26,27} near the boundary between the BoG and vortex liquid phases (see Fig. 2 of Ref. 27). From direct visualization of the flow of transport current in the system, it has been established²⁷ that the “vortex nanoliquid” is characterized by the simultaneous presence of solid- and liquid-like regions in the system. This phase is distinguished from the homogeneous vortex liquid by the presence of interconnected “droplets” of vortex liquid caged inside a solid matrix formed by other vortices. The experiments can not determine the positions of the droplets of vortex liquid relative to the grain boundaries that are known to exist in the BoG phase. This information is

provided by our earlier numerical studies^{28,29} of the vortex system. These studies reproduce all the experimentally observed features and in addition, show that the liquid regions in the “vortex nanoliquid” phase lie along the grain boundaries (see, for example, Fig. 7 of Ref. 29). Since the vortex liquid corresponds to the superfluid in the bosonic system, these results establish that a zero-temperature two-dimensional system of bosons, interacting via a repulsive pair potential proportional to $K_0(r)$ and in the presence of a small concentration of attractive pinning centers, exhibits a polycrystalline phase with superfluidity along the grain boundaries for a suitable choice of system parameters. In the present study, we examine whether this behavior persists in the bosonic system when the pinning potential is turned off, and calculate how the rotational inertia of the system is affected by the presence of droplets of superfluid lying along the grain boundaries.

B. Methods

Since our results for the bosonic system are obtained from studies of a system of vortices using the methods of our earlier work^{28–30}, we provide here a summary of the vortex model we consider and the numerical method we use to study its equilibrium behavior. The details of both the model and the method of calculation may be found in Ref. 35.

The system studied consisted of a set of vortex lines in a highly anisotropic, layered superconductor with the magnetic field perpendicular to the layers. The vortex lines are formed by stacks of “pancake” vortices located on the layers. The Josephson interaction between pancake vortices on different layers was neglected. The structure and thermodynamic properties of the vortex system are determined from numerical minimization of a model free energy functional of the Ramakrishnan-Yussouff form³⁶ that expresses the free energy of the system as a functional of the time-averaged local density of the pancake vortices. For columnar pins perpendicular to the layers, the pinning potential is the same on all the layers. This implies that the time-averaged density distribution is also the same on all the layers. This makes the problem effectively two-dimensional³⁵. Different phases of the vortex system correspond to different local minima of the free energy and phase transitions are signalled by crossings of the free energies of different local minima. From the density distribution at a local minimum representing a particular phase of the system, the positions of the vortices in that phase are generated by locating the points at which the density exhibits local peaks. This allows the study the real-space structures of different phases. The heights of the local density peaks are used to determine whether the vortices in a region of the sample are in a solid or liquid state.

Since our method of calculation is designed for the vortex system, the parameter that we control is the temper-

ature T of the vortex system. Changing this temperature is equivalent to “changing the value of \hbar ” in the corresponding zero T bosonic system via the mapping Eq. (2.4). This should be interpreted as changing system parameters in such a way that the relative importance of quantum effects is modified (“increasing \hbar ” implies increasing the importance of quantum fluctuations). This correspondence should be kept in mind in the interpretation of our results in the context of the bosonic problem.

III. RESULTS

As mentioned above, all our results for the two-dimensional bosonic system have been obtained from numerical calculations carried out for the equivalent vortex system. In our earlier studies^{28–30}, we considered a system of vortex lines in the presence of randomly placed columnar pinning centers and found polycrystalline BoG states when the areal density of the pinning centers is much smaller than that of the vortex lines. Since quenched disorder arising from the presence of pinning centers is not present in the ^4He samples studied experimentally in the context of supersolid behavior, we first investigated whether the polycrystalline states found in our earlier studies survive when the random pinning potential is turned off.

We use for this purpose two of the vortex configurations obtained and studied in Ref. 30. These correspond to results for a relative concentration $c = 1/8$ of columnar pins ($c = n_p/n_v$ where n_p , n_v are, respectively, the areal densities of pinning centers and vortex lines) in a system that contained 4096 vortices (therefore 512 columnar pins). We consider, for our starting point, vortex configurations at a vortex temperature $T = 17.0\text{K}$ at which point (for $c = 1/8$) the vortex system is well into the BoG phase, see the phase diagram in Fig. 1 of Ref. 30 (to set the temperature scale, we note that when no pinning is present, the vortex system considered undergoes a first-order melting transition from a crystalline Abrikosov lattice to a vortex liquid at $T = 18.4\text{K}$.) A perfectly crystalline state without grain boundaries is the absolute minimum of the free energy in the absence of pinning. However if, using the polycrystalline BoG configuration as a starting point, one reduces the strength of the pinning potential to zero in sufficiently small steps while running at every step the free-energy minimization routine, one ends up, when zero pinning strength is finally reached, with a *polycrystalline* sample, with well-defined grain boundaries. This polycrystalline state is of course metastable, but we find that as it is warmed up (we use steps of 0.2K), the sample remains in the local polycrystalline free energy minimum (within the finite accuracy of our numerical minimization procedure) until near $T = 18.4\text{K}$ when, as mentioned above, the microcrystals melt. Even if these polycrystalline states are not true local minima of the free energy, they can be made so by the introduction of a few pinning centers that are always

present in any physical sample.

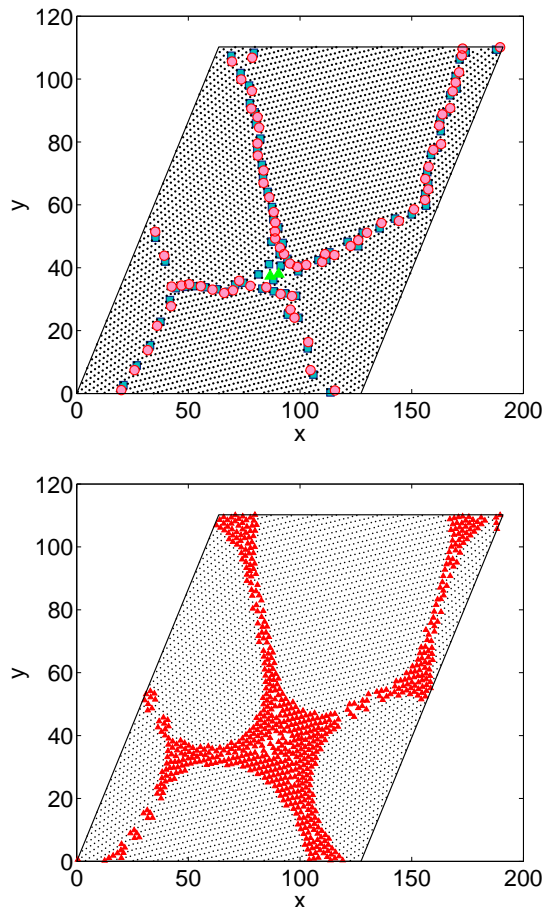


FIG. 1: (Color online) A metastable polycrystalline vortex configuration obtained as explained in the text. The temperature of the vortex system is $T = 18.2$ K, slightly below the melting temperature of the crystalline solid. Distances are in units of a_0 (see text). The top panel shows the results of a Voronoi construction (see text) that brings out the details of the polycrystalline structure. In this plot, vortices with 4, 5, 6 and 7 neighbors are shown as (green) triangles, (red) circles, (black) dots and (blue) squares, respectively. Adjacent pairs of 5- and 7-coordinated sites correspond to dislocations which line up along the grain boundaries that separate the microcrystals. The bottom panel shows the degree of localization of the vortices in the same configuration. Here, (red) triangles and (black) dots respectively represent liquid-like (less localized) and solid-like (strongly localized) vortices. This plot illustrates the phenomenon of premelting along the grain boundaries.

An example of such polycrystalline configurations, obtained by warming up the polycrystalline state originally obtained at a vortex temperature $T = 17.0$ K to 18.2 K, is shown in Fig. 1. There we plot the average positions of the vortices, defined to be the computational lattice sites at which the density has a local maximum. In this and subsequent figures, the unit of length is a_0 , defined by the relation $\pi a_0^2 n_v = 1$ where n_v is related to the magnetic

induction B (which was $B = 0.2T$ in the case shown) by $n_v = B/\Phi_0$ where Φ_0 is the superconducting flux quantum. In the top panel, we have shown the results of performing a Voronoi construction for the vortex configuration. The Voronoi cell associated with a lattice point is the region of space nearer to that point than to any other lattice point and the number of sides of the Voronoi cell represents the number of neighbors of the lattice point. In the top panel, vortices with six neighbors are shown as (black) dots and those with five or seven neighbors are shown as (red) circles and (blue) squares respectively. A neighboring pair of five- and seven-coordinated vortices constitutes a dislocation and grain boundaries correspond to arrays of such dislocations. Microcrystals can be seen as ordered regions consisting of sites with six neighbors, and these microcrystals are separated by arrays of dislocations (pairs of sites with five and seven neighbors) denoting the grain boundaries.

In the bottom panel of Fig. 1, we show, for the same configuration, the spatial distribution of the value of the vortex density at each local density peak, normalized to the average vortex density value n_v . The value of this dimensionless quantity provides a measure of the degree of localization of the corresponding vortex. Using the value of this quantity, we can determine whether the vortices in a given region are liquid- or solid-like. In our earlier studies of the vortex system^{28–30} (see, for example, Sec. IIIC of Ref. 30, or Sec. IIID of Ref. 29), we found that vortices in liquid regions correspond to local density peaks for which this quantity has values of three or less, while those with higher values of this quantity correspond to solid regions. In the plot, local density peaks representing solid and liquid regions according to this quantitative criterion are denoted as (black) dots and (red) triangles, respectively. One can see that all the vortices in the ordered regions are solid-like: these regions correspond to microcrystals. In contrast, the vortices near the grain boundaries form liquid channels that separate the microcrystals. This plot illustrates the occurrence of a kind of “premelting” in the regions near the grain boundaries: these regions melt and become liquid-like (superfluid in the equivalent bosonic system) at temperatures lower than that at which the bulk crystal melts (which we recall is 18.4 K). Premelting along grain boundaries is well-known³⁷ in classical solids. Our observation of this phenomenon in the vortex system is consistent with experimental results. At lower temperatures, the liquid channels along the grain boundaries are narrower and obstructed at the narrowest spots (see Fig. 2 below for an example), forming a chain-like structure of small liquid droplets. As the temperature is reduced further, the liquid regions near the grain boundaries disappear completely and are replaced by narrow strips of disordered solid.

These results imply, from the vortex-boson mapping, that a two-dimensional polycrystalline system of bosons exhibits superfluidity along grain boundaries over a suitable range of parameter values. Using the realistic net-

works of grain boundaries obtained from our numerical studies of the vortex system, we can then investigate how the NCRI arising from the presence of superfluid channels in the bosonic system depends on the system parameters. The numerically obtained samples in themselves are too small to allow a realistic study of the flows, but a sufficiently, indeed arbitrarily large, sample can be obtained from them through periodic repetitions (periodic boundary conditions are used in our original numerical studies) that produce a tiling of a larger region with the smaller samples. One obtains then a larger sample for which the short-distance structure is the same, but which has a different large-scale structure because longer liquid channels are produced when different copies of the original sample are juxtaposed. Indeed, the length of the largest channels after such a juxtaposition is of the order of that of the combined sample. It is true that the structure of the original small sample is preserved in the small-scale structure of the large sample, which has an artificial periodicity. However, this is not important: the behavior of the moment of inertia of the liquid region, and therefore the NCRI is of course determined essentially by the largest-scale channels in the problem. Scaling the system by a linear factor of $s > 1$ in this way introduces liquid channels that are larger by a factor of up to s than the original ones, while leaving the original small-scale structures and the channel widths unchanged. It follows from geometrical and similarity considerations that the overall moment of inertia of the channels, including the contributions from the additional smaller structures, should then scale as s^4 . Hence, our conclusions for the moments of inertia, which we will normalize to the overall rigid-body value, which also scales in the same way, will be independent of this procedure. The samples considered in our NCRI calculations are selected portions of 3×3 tilings of the originally obtained samples.

The evolution of the network of liquid channels in one of these samples with increasing temperature T of the vortex system is displayed in Fig. 2. Each panel shows a different value of T ranging from $17.8K$ to $18.4K$. In these plots, vortices in the liquid regions are shown as (blue) squares, and those in the solid regions as (black) dots. At the lowest temperature, $T = 17.8K$, the liquid regions form largely disconnected, small beads located along the grain boundaries, with larger droplets forming at the intersections of two grain boundaries. As T is increased, the bead-like liquid structures coalesce into channels, so that at about $T = 18.2K$, connected structures of size comparable to that of the whole sample (in particular, a ring-like structure that can be seen in the upper left corner of the figure) appear. Finally, at $T = 18.4 K$, just below the melting temperature of the vortex solid, the liquid regions have fully developed into open channels which percolate through the sample. As the superfluid in the equivalent bosonic system is allowed, in the configurations obtained in the higher T range, to freely flow along these channels, whose characteristic size is now of the order of the sample size, it is clear that the

moment of inertia will exhibit a substantial reduction, leading to appreciable values of the NCRI.

To numerically calculate the moment of inertia of the bosonic samples, we proceed as follows: we imagine the microcrystalline sample rotating about its center of mass, with angular speed Ω . The solid regions of the sample, composed of the microcrystals, rotate of course as a rigid body with the angular velocity Ω . The material in the liquid (superfluid in the bosonic system) channels will flow according to a pattern that can be determined by numerically solving the fluid flow equations of an incompressible, irrotational (super)fluid.^{33,34} These equations can be solved to obtain the velocity field $\mathbf{v}(\mathbf{r})$ in the fluid regions. The velocity field at the boundaries of the fluid part of the sample must satisfy the boundary condition³³ that follows from assuming that the fluid is confined by the rigid walls. This implies that the component of the velocity field $\mathbf{v}(\mathbf{r})$ along the outward normal $\hat{\mathbf{n}}$ at any point on the boundary must be equal to the component of the rigid-body velocity $\Omega \times \mathbf{r}$ along $\hat{\mathbf{n}}$ at that point:

$$\mathbf{v}(\mathbf{r}) \cdot \hat{\mathbf{n}} = (\Omega \times \mathbf{r}) \cdot \hat{\mathbf{n}} \quad (3.1)$$

where \mathbf{r} is a vector from the center of rotation to a point on the liquid region boundary. In addition, if the fluid region is not simply connected, then the circulation of the velocity field along a closed path surrounding each inner boundary of the region must be specified in order to make the problem well-defined³⁸. We assume that the sample is accelerated from rest at zero temperature, so that the values of these circulations are zero³⁹. Once the velocity field is obtained, the resulting angular momentum, and hence the moment of inertia can be straightforwardly obtained by numerical integration.

Analytic solution of this problem is feasible^{33,34} only for reasonably simple geometries: for the very irregular geometries involving the multiple channels and regions under study here solution can only be undertaken numerically. The numerical method we have used involves spatial discretization and iterative relaxation⁴⁰ to obtain a solution of the Laplace equation (see below) with appropriate boundary conditions. There are certain technical difficulties involved in doing this. The main one is that our definition of whether a part of the sample is solid or liquid is based on the values of the density at the local peaks which form a discrete lattice. This lattice must therefore be our computational lattice for the purpose of calculating the velocity field and the moment of inertia and we cannot truly gain additional precision by adding more points. Any attempt to do so would necessarily involve some non-controllable interpolation scheme. This unavoidable situation leads to some uncertainties in our numerical results. In particular, the final results for the rotational inertia include some numerical uncertainty arising from this minimum spacing of our computational lattice. Another technical difficulty is that the boundary condition for the velocity field, Eq.(3.1), is of the Neumann form if one uses the standard method^{33,34} to

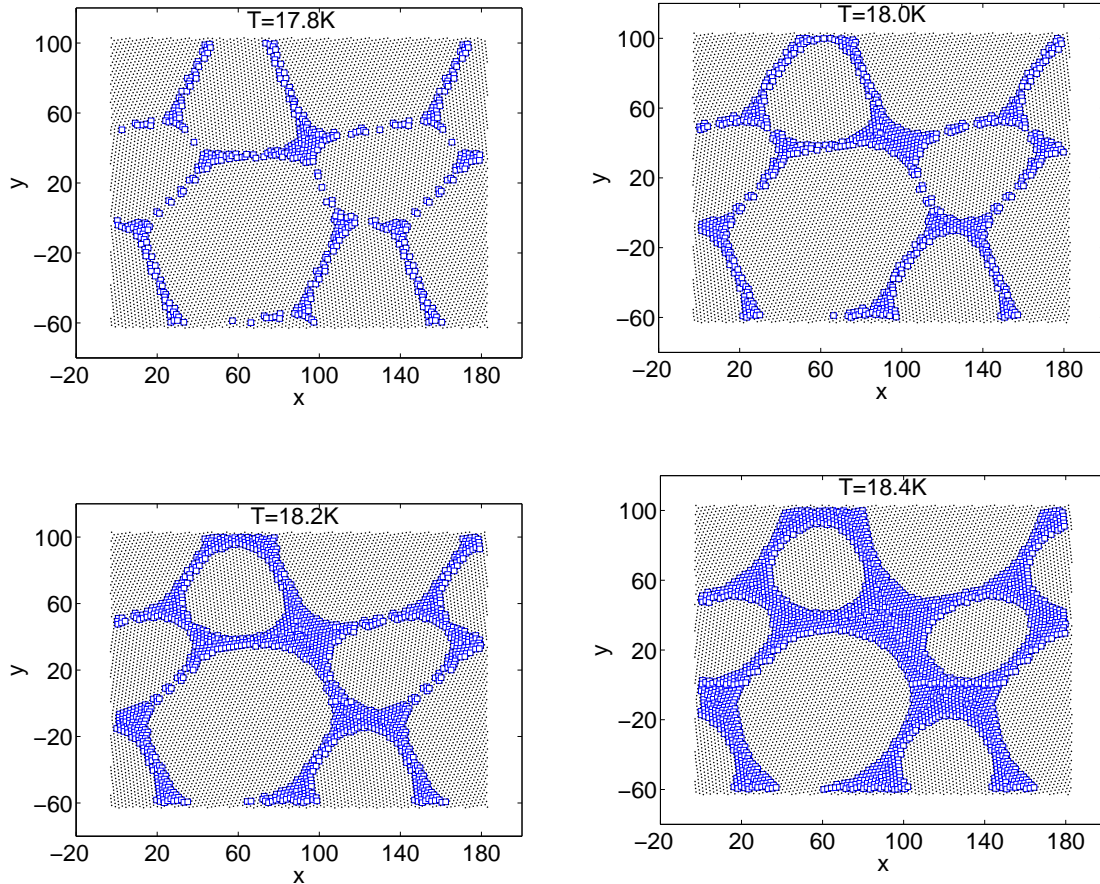


FIG. 2: (Color online) Evolution of the network of liquid channels with the temperature T of the vortex system in one of the samples studied. Each of the four panels corresponds to a value of T as indicated. Vortices in liquid regions are shown as (blue) squares and those in the microcrystal are shown as (black) dots. One can see that as T increases, the liquid channels become connected and closed loops of size comparable to that of the sample are formed. Units of length are as in Fig. 1.

express the incompressible velocity field $\mathbf{v}(\mathbf{r})$ as

$$v_x(\mathbf{r}) = -\partial\Psi(\mathbf{r})/\partial y, \quad v_y(\mathbf{r}) = \partial\Psi(\mathbf{r})/\partial x, \quad (3.2)$$

in terms of a stream function $\Psi(\mathbf{r})$. The simplification of replacing the boundary condition of Eq. (3.1) by the Dirichlet boundary condition, $\Psi(\mathbf{r}) = \frac{1}{2}\Omega r^2$, at all points on the boundary, which was used in earlier studies^{33,34}, works for some simple geometries, but leads to incorrect results when unobstructed ring-like channels are present. This can be easily checked by applying this method to determine the velocity field in a superfluid confined between two concentric cylinders rotating about their common axis. This forces us to use the original Neumann boundary conditions of Eq. (3.1). These are more difficult and awkward to implement numerically, as they involve the outward normal $\hat{\mathbf{n}}$ at the boundary, which can be defined in different ways when the boundary consists of a set of discrete points. With the possibility of reducing the computational lattice spacing not being available to us, this introduces additional numerical uncertainty,

as the final results are somewhat sensitive to the way in which $\hat{\mathbf{n}}$ is defined. However, these uncertainties do not seriously affect the quantitative conclusions that we can draw from our calculation, as we shall see below. We recall that using a scalar potential for the velocity field leads to other undesirable problems³⁴ even in some analytic cases.

The irrotational nature of superfluid flow in the absence of any superfluid vortex implies that $\nabla \times \mathbf{v} = 0$ in the superfluid regions. This condition and the definition of the stream function Ψ in Eq.(3.2) imply that Ψ must satisfy the Laplace equation, $\nabla^2\Psi(\mathbf{r}) = 0$, inside each superfluid channel. Using a triangular computational grid of spacing equal to the average inter-particle distance and representing the Laplace operator by symmetric differences⁴⁰, the Laplace equation can be reduced to a set of linear equations satisfied by the values of Ψ at the computational grid points in the interior of each superfluid region. The boundary conditions of Eq.(3.1) can also be written as a set of linear equations involving

the values of Ψ at the grid points on the boundary of a superfluid region and their nearest neighbors. This set of coupled linear equations is numerically solved using iterative relaxation⁴⁰. This yields the values of Ψ at the grid points, from which the velocity field and the rotational inertia can be easily obtained.

In Fig. 3, we present what is the main result of these computations for the NCRI. The quantity plotted there (circles) as a function of temperature T (which, we reiterate, is the temperature at which the calculations for the vortex system were performed – it should not be confused with the temperature of the equivalent bosonic system which is zero) is the NCRIF, defined as the difference between the moment of inertia of the entire sample as a rigid body and its actual moment of inertia when the superfluid flow in the liquid portions is taken into account, normalized by the total rigid-body moment of inertia. These results are for the sample shown in Fig. 2. At lower temperatures, when the liquid regions form small, disconnected clusters (see the discussion above in connection with Fig. 2), the superfluid flow is negligible and the entire system behaves as a rigid body, so the value of the NCRIF is very close to zero. At higher temperatures, when the disconnected liquid regions join together to form extended channels, superfluid flow begins to occur over relatively large portions of the sample and eventually the characteristic channel length becomes of the order of the system size. At $T = 18.2K$, a large, ring-like channel opens up (see Fig. 2), providing a closed path for the flow of the superfluid. This drastically reduces the moment of inertia; recall for example that the moment of inertia of a superfluid confined in a ring that is rotating about its center is zero. Therefore the NCRIF increases very drastically (note the logarithmic vertical scale) and by the time the temperature is reached where the channels are fully open, it has increased by nearly three orders of magnitude, while of course remaining relatively small ($\sim 5\%$). Our conclusion about a rapid increase in the value of the NCRIF at $T = 18.2K$, when a large, ring-like channel opens up to allow the flow of the superfluid along a closed path, is not affected by the above mentioned uncertainties in the numerical results, which are $\sim 25\%$ in the worst case. We have repeated the whole calculation for a second polycrystalline configurations and obtained very similar results. Specifically, we find in both cases that the NCRIF increases by a factor of ~ 18 at $T = 18.2K$ when a large, ring-like liquid channel opens up.

In Fig. 3, we have also shown (triangles) the dependence of f , the fraction of the sample that is liquid-like (superfluid in the bosonic system), on T . It is clear from this plot that the dependence of this quantity on T is qualitatively different from that of the NCRIF: the liquid fraction f increases smoothly with increasing T and does not exhibit the rapid increase seen in the NCRIF at $T = 18.2K$. This observation brings out the important point that the NCRIF may not provide a good measure of the fraction of superfluid regions of the system

if the superfluidity occurs along a network of channels – the connectivity of the channels plays an important role in determining the value of the NCRIF. The NCRIF remains small as long as the network does not contain large ring-like paths along which the superfluid can flow without any blockage. The first opening up of such paths as some system parameter is varied leads to a large increase in the value of the NCRIF. This large increase, which may look like the onset of superfluidity, does not necessarily correspond to a sudden, large increase in the superfluid fraction f of the system. This should be kept in mind while interpreting experimental data for the NCRIF.

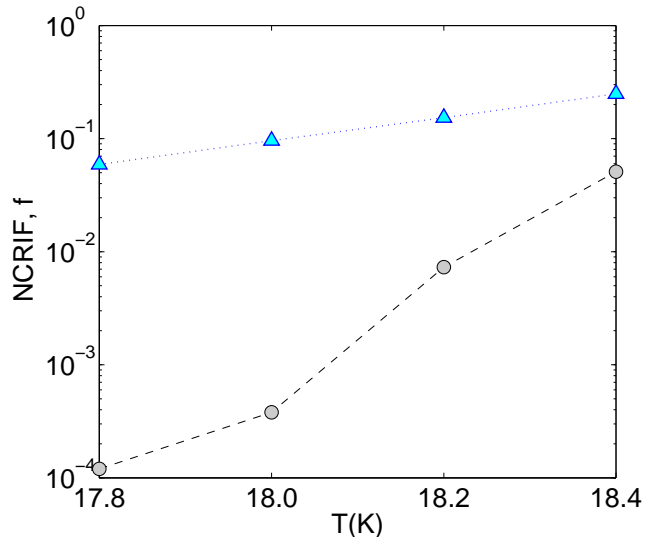


FIG. 3: The NCRIF, calculated and normalized as explained in the text, plotted as a function of T , the temperature of the vortex system (circles). Also shown are the values of f , the liquid (superfluid in the bosonic system) fraction (triangles). The straight line segments join consecutive data points.

IV. SUMMARY AND DISCUSSIONS

In this work, we have studied the NCRI arising from superfluidity along grain boundaries in a two-dimensional bosonic system at zero temperature. By making use of standard mappings, we have related the properties of the bosonic system to those of a system of superconducting vortex lines at finite temperatures. The latter system has been extensively studied by numerical methods and computationally obtained structures in the different phases it can exhibit are available. One of the possible structures of this vortex system is a polycrystalline solid in which liquid regions near the grain boundaries between microcrystals expand and form more connected regions which eventually extend through the sample as the vortex system temperature is increased. These vortex configurations, obtained from previous numerical studies, correspond, via the above mentioned mappings, to different

configurations of the boson system, each containing more or less extensively connected narrow superfluid regions, separating much larger and compact crystalline regions. We have then calculated the moment of inertia of the bosonic samples by numerically solving the equations of superfluid hydrodynamics in the superfluid regions of the sample.

We have found that the non-classical portion of the moment of inertia of such samples (the NCRIF) is nearly zero as long as the vortex liquid (bosonic superfluid) regions remain disconnected, but it increases abruptly by about two orders of magnitude as the superfluid channels become connected to form ring-like structures with sizes comparable to the system size. The values we find for the fully developed NCRIF are of the order of a few percent. Thus, our results indicate that NCRI behavior can indeed arise in two-dimensional bosonic systems from superfluid regions associated with grain boundaries. The magnitude of the jump in the NCRIF and the final NCRIF values obtained from our calculations are quite similar to what is found experimentally in solid ^4He . Our results, therefore, lend support to the notion that supersolid phenomena in ^4He are related to superfluidity in grain boundaries or other crystal defect regions, such as dislocations. Our results also indicate that an abrupt increase in the NCRIF from a vanishingly small value to a few percent does not necessarily correspond to a similar increase in the fraction of the sample that is superfluid. As shown in Fig. 3, such an increase in the NCRIF may actually correspond to the opening up of system-spanning ring-like channels through which the superfluid can flow without any block. The importance of the existence of a percolating network of superfluid channels in observing macroscopic signatures of superfluidity has been pointed out in an earlier study²¹. However, we are not aware of any calculation of the behavior of the NCRIF across the percolation transition.

As discussed above, the results of existing experimental^{25–27} and numerical^{28–32} studies of vortex lines with dilute columnar pinning strongly suggest, via the mapping used here, that a polycrystalline state with superfluidity along grain boundaries occurs in a two-dimensional bosonic system with a small concentration of strong pinning centers. Such a state may be seen in experiments⁴¹ on films of ^4He adsorbed on substrates with imperfections that act as pinning centers. In the vortex system, the equilibrium phase changes from polycrystalline Bose glass to vortex nanoliquid and then to homogeneous liquid as the temperature is increased. In the equivalent bosonic system, this sequence corresponds to going from a polycrystalline solid to a “supersolid” with superfluidity in the grain boundary regions and then to a homogeneous superfluid. It is, however, not clear how the experimentally accessible parameters in the bosonic system can be changed to simulate the effects of increasing the temperature in the vortex system. The same sequence of phases can also be seen^{25–27} in the vortex system by increasing the magnetic induction at a fixed, low temper-

ature. Since the magnetic induction in the vortex system determines the areal density of the vortex lines, the supersolid phase in a two-dimensional bosonic system may be accessed by changing the coverage of the ^4He film. The supersolid would be the true equilibrium phase of the system when random defects are present. Our numerical results, furthermore, suggest that the supersolid survives as a metastable phase even in the absence of random pinning. While it is not obvious how such a metastable phase could be accessed in experiments, the supersolid behavior observed in three-dimensional solid ^4He must also be a metastable phenomenon if it arises from superfluidity in a network of structural defects, because these defects would not be present in the true equilibrium solid which should be a perfect crystal.

In making any comparison of the behavior of the bosonic system found in our study with experiments on ^4He samples, one should keep in mind the important fact that the interaction between two ^4He atoms (strongly repulsive at short distances, with a weak attractive part at larger distances that falls off with distance as a power-law) is substantially different from that between two bosonic particles in the system considered here (purely repulsive, logarithmic at short distances and exponentially decaying at longer distances). For this reason, the results of our study can not be applied quantitatively to experimentally studied ^4He systems. However, we expect the qualitative behavior found in our study to be observed in systems of ^4He atoms because the phenomena on which our conclusions are based (i.e. the formation of polycrystalline structures and “pre-melting” along grain boundaries) are fairly generic, independent of the details of the inter-particle potential.

In experiments on ^4He , a normal solid to supersolid transition is observed^{1–9} as the temperature of the sample is decreased. So, it is interesting to inquire whether our study provides any information about the behavior of the bosonic system as *its* temperature is changed. Unfortunately, we can not address this experimentally relevant question in our study. This is because a nonzero temperature in the bosonic problem maps to a vortex system of finite thickness L , and our studies of the vortex system, carried out for the $L \rightarrow \infty$ limit, do not provide any information about phase changes that may occur as L is varied at constant temperature.

We close with a discussion of whether the available experimental results for supersolid ^4He show any evidence for the sequence of phases (polycrystal to vortex nanoliquid to vortex liquid) found in the vortex system upon increasing its temperature T . In the equivalent bosonic system, this sequence corresponds to a transition from a defected solid to a supersolid, followed by a second transition from the supersolid to a superfluid. The vortex-boson mapping implies that increasing T in the vortex problem is equivalent to increasing the relative importance of quantum effects in the zero-temperature boson problem. It has been suggested^{42,43} that increasing the pressure P has the effect of reducing the relative impor-

tance of quantum fluctuations in solid ^4He . Assuming this to be correct, increasing (decreasing) T in the vortex system should be analogous to *decreasing (increasing)* P in ^4He experiments. Then the relevant question is whether a sequence of normal solid to supersolid to superfluid transitions occurs in ^4He as P is decreased at constant temperature. There is some experimental evidence⁴³ for a reduction in the low-temperature value of the apparent superfluid fraction in supersolid ^4He as P is increased beyond 55 bar. This may correspond to a transition from the supersolid to a regular defected solid, analogous to the disappearance of the liquid regions in the vortex system as T is decreased. Also, the “phase diagram” of ^4He in the $P - T$ plane shown in Ref. 1 suggests that the temperature of the normal solid to supersolid transition decreases as P is increased (the transition temperature is found to decrease from 315 mK at

a pressure of 26 bars to 230 mK at pressures exceeding 40 bars). If this relatively weak dependence of the transition temperature on pressure is a genuine effect, then decreasing P at constant T would indeed lead to a sequence of two transitions, first from the normal solid to the supersolid and then from the supersolid to the superfluid phase. This would be analogous to the behavior seen in our calculations. More detailed investigations of the pressure-dependence of supersolid behavior in ^4He would be very interesting in this context.

Acknowledgments

This work was supported in part by NSF (OISE-0352598) and by DST (India).

-
- * Electronic address: cdgupta@physics.iisc.ernet.in; Also at Condensed Matter Theory Unit, Jawaharlal Nehru Centre for Advanced Scientific Research, Bangalore 560064, India
- † Electronic address: otvalls@umn.edu; Also at Minnesota Supercomputer Institute, University of Minnesota, Minneapolis, Minnesota 55455
- ¹ E. Kim and M.W.H. Chan, *Science* **305**, 1941 (2004); *Phys. Rev. Lett.* **97**, 115302 (2006).
 - ² A. C. Clark, J.T. West and M. W. H. Chan, *Phys. Rev. Lett.* **99**, 135302 (2007).
 - ³ See S. Balibar and F. Caupin, *J. Phys. Condens. Matter* **20**, 173201 (2008) for a review.
 - ⁴ A. S. C. Rittner and J.D. Reppy, *Phys. Rev. Lett.* **97**, 165301 (2006); *ibid.* **98**, 175302 (2007).
 - ⁵ Y. Aoki, J.C. Graves and H. Kojima, *Phys. Rev. Lett.* **99**, 015301 (2007).
 - ⁶ A. Penzev, Y. Yasuta, and M. Kubota, *J. Low Temp. Phys* **148**, 667 (2008).
 - ⁷ M. Kondo, S. Takada, Y. Shibayama, and K. Shirahama, *J. Low Temp. Phys.* **148**, 695 (2008).
 - ⁸ B. Hunt *et al.*, *Science* **324**, 632 (2009).
 - ⁹ J. Day and J. Beamish, *Nature* **450**, 853 (2007).
 - ¹⁰ A. F. Andreev and I. M. Lifshitz, *Sov. Phys. JETP* **29**, 1107 (1969).
 - ¹¹ B. K. Clark and D. M. Ceperley, *Phys. Rev. Lett.* **96**, 105302 (2006).
 - ¹² M. Boninsegni *et al.*, *Phys. Rev. Lett.* **97**, 080401 (2006).
 - ¹³ J.T. West, O. Syshchenko, J. Beamish and M.W.H. Chan, *Nature Physics* **5**, 598 (2009).
 - ¹⁴ L. Pollet, M. Boninsegni, A.B. Kuklov, N.V. Prokofiev, B. V. Svistunov, and M. Troyer, *Phys. Rev. Lett.* **98**, 135301 (2007).
 - ¹⁵ M. Boninsegni *et al.*, *Phys. Rev. Lett.* **99**, 035301 (2007).
 - ¹⁶ S.G. Soyler, A.B. Kuklov, L. Pollet, N.V. Prokofiev, and B. B. Svistunov, *Phys. Rev. Lett.* **103**, 175301 (2009).
 - ¹⁷ S. Gaudio, E. Cappelluti, G. Rastelli, and L. Pietronero, *Phys. Rev. Lett.* **101**, 075301 (2008); *ibid.* **104**, 049602 (2010).
 - ¹⁸ B. Yucsoy, J. Machta, N. Prokofiev, and B. Svistunov, *Phys. Rev. Lett.* **104**, 049601 (2010).
 - ¹⁹ S. I. Shevchenko, *Sov. J. Low Temp. Phys.* **14**, 533 (1988).
 - ²⁰ A.T. Dorsey, P.M. Goldbart and J. Toner, *Phys. Rev. Lett.* **96**, 055301 (2006).
 - ²¹ J. Toner, *Phys. Rev. Lett.* **100**, 035302 (2008).
 - ²² D. R. Nelson, *Phys. Rev. Lett.* **60**, 1973 (1988).
 - ²³ D.R. Nelson and V.M. Vinokur, *Phys. Rev. B* **48**, 13060 (1993).
 - ²⁴ A.I. Larkin and V.M. Vinokur, *Phys. Rev. Lett.* **75**, 4666 (1995).
 - ²⁵ M. Menghini *et al.*, *Phys. Rev. Lett.* **90**, 147001 (2003).
 - ²⁶ S.S. Banerjee *et al.*, *Phys. Rev. Lett.* **90**, 087004 (2003).
 - ²⁷ S.S. Banerjee *et al.*, *Phys. Rev. Lett.* **93**, 097002 (2004).
 - ²⁸ C. Dasgupta and O.T. Valls, *Phys. Rev. Lett.* **91**, 127002 (2003).
 - ²⁹ C. Dasgupta and O.T. Valls, *Phys. Rev. B* **69**, 214520 (2004).
 - ³⁰ C. Dasgupta and O.T. Valls, *Phys. Rev. B* **72**, 094501 (2005).
 - ³¹ Y.Y. Goldschmidt and E. Cuansing, *Phys. Rev. Lett.* **95**, 177004 (2005).
 - ³² Y.Y. Goldschmidt and J.-T. Liu, *Phys. Rev. B* **76**, 174508 (2007).
 - ³³ A.L. Fetter, *J. Low Temp. Phys.* **16**, 533 (1974).
 - ³⁴ C. Dasgupta and O.T. Valls, *Phys. Rev. E* **79**, 016303 (2009).
 - ³⁵ C. Dasgupta and O.T. Valls, *Phys. Rev. B* **66**, 064518 (2002).
 - ³⁶ T.V. Ramakrishnan and M. Yussouff, *Phys. Rev. B* **19**, 2275 (1979). otv
 - ³⁷ A.M. Alsayed, M.F. Islam, J. Zhang, P.J. Collings and A.G. Yodh, *Science* **309**, 1207 (2005), and references therein.
 - ³⁸ J.B. Mehl and W. Zimmermann, Jr., *Phys. Rev.* **167**, 214 (1968).
 - ³⁹ A. L. Fetter, *Phys. Rev.* **153**, 285 (1967).
 - ⁴⁰ P. W. Gash, *Am. J. Phys.* **59**, 509 (1991).
 - ⁴¹ P.A. Crowell and J.D. Reppy, *Phys. Rev. B* **53**, 2701 (1996).
 - ⁴² L.H. Nosanow, *Phys. Rev. Lett.* **13**, 270 (1964).
 - ⁴³ E. Kim and M.W.H. Chan, *Phys. Rev. Lett.* **97**, 115302 (2006).